Normalization of fringe patterns using the bidimensional empirical mode decomposition and the Hilbert transform

María B. Bernini,[1,*] Alejandro Federico,[2] and Guillermo H. Kaufmann[1,3]

[1]Instituto de Física Rosario, Boulevard 27 de Febrero 210 bis, S2000EZP Rosario, Argentina

[2]Electrónica e Informática, Instituto Nacional de Tecnología Industrial, P.O. Box B1650WAB, B1650KNA San Martín, Argentina

[3]Centro Internacional Franco Argentino de Ciencias de la Información y de Sistemas, Boulevard 27 de Febrero 210 bis, S2000EZP Rosario, Argentina

*Corresponding author: bernini@ifir-conicet.gov.ar

Received 2 June 2009; revised 14 October 2009; accepted 13 November 2009; posted 19 November 2009 (Doc. ID 112223); published 10 December 2009

We evaluate a data-driven technique to perform bias suppression and modulation normalization of fringe patterns. The proposed technique uses a bidimensional empirical mode decomposition method to decompose a fringe pattern in a set of intrinsic frequency modes and the partial Hilbert transform to characterize the local amplitude of the modes in order to perform the normalization. The performance of the technique is tested using computer simulated fringe patterns of different fringe densities and illumination defects with high local variations of the modulation, and its advantages and limitations are discussed. Finally, the performance of the normalization approach in processing real data is also illustrated.

OCIS codes: 120.2650, 120.3180.

1. Introduction

Optical interferometry is a widely known technique in scientific and industrial applications, and its use has been increased since the introduction of automated methods of fringe patterns analysis [1]. The aim of fringe pattern analysis is the extraction of some physical quantities from the optical phase distribution coded in one or several fringe patterns. Optical phase recovery techniques, especially in those measurement systems where the whole physical information is contained in a single fringe pattern, are very sensitive to modulation defects that are mostly due to nonuniform illumination. Consequently, the fringe pattern to be analyzed must be usually normalized before the phase map is extracted in order to avoid the introduction of large errors in the phase demodulation process.

Recently, several fringe normalization techniques have been proposed. In Ref. [2], two orthogonal bandpass filters are combined to obtain an estimate of the normalized modulation intensity. This method has been successfully applied in fringe normalization, although its efficiency is reduced in images with very low modulation regions or stepped contrast changes. More recently, a technique based on a quadrature operator using one-dimensional (1D) Reisz filters was presented [3]. This technique is especially designed for n-dimensional fringe patterns and needs to preprocess the fringe pattern to remove the bias term. In phase recovering processes from a single fringe pattern the application of the regularized phase tracking (RPT) technique is also known. In Ref. [4], a normalization step was added to this technique consisting of the addition of one term to the RPT

0003-6935/09/366862-08$15.00/0

function that models the fringe pattern modulation. This approach is quite useful in fringe patterns with high frequency noise, although it is necessary to preprocess the fringes to remove the bias term, and it also requires a long processing time.

Digital speckle pattern interferometry (DSPI) is an important coherent optical technique widely used for whole-field measurement of displacements, strain fields, and contours in rough objects [5]. Fringe patterns generated in DSPI are usually produced by the correlation of two or more speckle interferograms created by different deformation states of the object under study. Phase extraction procedures from single DSPI fringe patterns is a complex task, usually due to the residual speckle noise [6–9]. Therefore, a speckle denoising technique to smooth the DSPI fringes must be previously applied to phase extraction [10,11]. However, the use of a smoothing preprocess usually reduces fringe visibility or can introduce oversmoothing, so that a normalization technique must be applied before the phase distribution is retrieved. Recently, a technique was presented for filtering and normalizing a fringe pattern by means of an iterative procedure based on the construction of an adaptive filter as a linear combination of isotropic bandpass filters [12]. With the same purpose, in another recently introduced approach an expression of the cosine profile of the fringe pattern is formulated and based on the use of directional derivatives [13]. However, it was observed that the obtained results can be severely affected if the analyzed fringe pattern contains very low modulation regions or stepped contrast changes as in the case of the technique presented in Ref. [2].

In this paper we evaluate a data-driven approach to normalize fringe patterns containing very low noise levels or previously denoised fringes and also to remove its bias term using the bidimensional empirical mode decomposition (BEMD) method, similar to the one described in Ref. [14], and the partial Hilbert transform (PHT). BEMD is a two-dimensional (2D) extension of the empirical mode decomposition (EMD) method first introduced by Huang [15]. EMD is an adaptive technique that decomposes nonstationary and nonlinear 1D signals in a finite number of fast and slow oscillations of zero mean called intrinsic mode functions (IMFs). BEMD is used to decompose images in a small group of 2D IMFs and a residual image. This decomposition is carried out through a fully data-driven sifting process, so that no basis functions need to be fixed.

The technique proposed in this paper performs bias removal and modulation normalization of fringe patterns in a single process. In addition, the computational time is not demanding. In this approach, a fringe pattern is first decomposed by using the BEMD technique, then the amplitudes of the first significative 2D IMFs are calculated by using the PHT. The normalized fringe pattern is finally obtained by adding the significative 2D IMFs divided by its respective amplitude. The rest of the decomposition contains the bias component that is automatically removed.

In the following sections we briefly explain the theoretical concepts of BEMD and the PHT. We also describe the proposed normalization technique and test its performance on computer-simulated fringe patterns by using a quality index. Finally, an application of the proposed technique to normalize an experimental DSPI fringe pattern is presented, and the obtained results are also compared with those given by the approach presented in Ref. [2].

2. Theoretical Concepts

A. BEMD Method

The BEMD method is an adaptive and data-driven technique that decomposes an image into a small set of subimages called 2D IMFs, representing the high and low frequency components of the original image and a residue. There are some conditions that a bidimensional function must meet to be a 2D IMF: (1) the mean value between the envelopes defined by the local maxima and minima of a 2D IMF is close to zero everywhere; (2) the number of extrema and zero crossings must be approximately the same. The residue is a bidimensional function that has less than three extrema. The 2D IMFs are defined by the fringe pattern itself using a sifting process defined as follows:

1. Initialization: $h = I$, where I is the fringe pattern to be analyzed (input image).
2. Find all local maxima and minima of image h.
3. Generate the upper and lower 2D envelopes by connecting all local extrema.
4. Calculate the mean function Envmean of the upper and lower 2D envelopes.
5.. Subtract Envmean from the input image and $h \equiv h$ – Envmean.
6. Repeat the process until the stop criterion is met and h is a 2D IMF.

The next step of the decomposition process consists of subtracting the obtained h from the input image. The residue of this subtraction is used as the new input image, and all the sifting process is repeated until no more 2D IMFs can be obtained. The process is ended when the number of extreme points is less than three. The last input data of the algorithm do not meet the conditions to be a 2D IMF and are called the residue. Once the decomposition is completed, the input image I is reconstructed as the sum of all the 2D IMFs and the residue.

The procedures utilized for extrema detection and the interpolation to generate the upper and the lower 2D envelopes used in this work are similar to those applied in Ref. [14]. Local maxima and minima were extracted using the 4-connected neighbors method. According to this method, a value $I(x, y)$ is a local maxima (or minima) of the image I if is larger (or lower) than its 4-connected neighbors [16]. The

technique selected for maxima and minima interpolation was a triangle-based cubic spline interpolation. This method is based on the Delauney triangulation of the maxima and minima and piecewise cubic interpolation on triangles [17]. This interpolation technique is usually applied due to its low computational cost when images with a large number of extreme points need to be processed [16,18]. The interpolated surface must connect every data point and the second derivative must be continuous everywhere, so that the surface is smooth enough. For this reason, the BEMD method strongly depends on the interpolation technique used to generate the envelopes.

The criterion adopted to stop the sifting process was the normalized standard deviation SD used in Ref. [14], being

$$\mathrm{SD} = \frac{\sum_{x=1}^{x=X}\sum_{y=1}^{y=Y}|h_{ik-1}(x,y) - h_{ik}(x,y)|^2}{\sum_{x=1}^{x=X}\sum_{y=1}^{y=Y}h_{ik-1}^2(x,y)} < \varepsilon, \quad (1)$$

where $X \times Y$ is the number of samples of the image, i is the index corresponding to the ith 2D IMF, and k is the step number of the sifting process. After carrying out numerous tests, it was verified that a value of ε between 0.02 and 0.08 was suitable for the type of fringe patterns analyzed in this work.

The errors generated in the boundaries during the sifting process can be spread inwards through the 2D IMFs causing severe drawbacks. Several authors have addressed this issue in EMD [15,19,20] and BEMD [18,21,22] using diverse approaches, such as by adding data in the borders by reflection and also by symmetrization through the edges of the image. However, there are no standard solutions to deal with this issue. Here, we introduced a boundary extension of the fringe patterns to be normalized in order to avoid the error propagation inwards the 2D IMFs. A linear predictive extrapolation method was used in order to perform this preprocessing, in which the phase and frequency of the signal are maintained [23]. Linear prediction consists of estimating new values from a signal as a linear function of previously known ones. In this case, we extrapolate the values of the boundaries using the values of each line of the image to generate the extended border. The length of the used extension in each direction is half of the fringe pattern. After the decomposition, only the central parts of the extended 2D IMFs that correspond to the original size of the fringe pattern were used.

B. Normalization Method

As previously mentioned, the technique proposed in this paper performs both bias suppression and modulation normalization in a single process. The modulation normalization is performed by decomposing a fringe pattern with the BEMD method in order to obtain the first significant 2D IMFs. Then, the amplitude of the selected 2D IMFs is calculated using the PHT.

The PHT of a 2D IMF (or a set of added 2D IMFs), named $I_{\mathrm{IMF}}(x,y)$, is defined as the Hilbert transform with respect to each of the coordinates [24]. The partial Hilbert transform of $I_{\mathrm{IMF}}(x,y)$ with respect to the coordinate x is defined by

$$H_x(x,y) = \frac{1}{\pi}\mathrm{PV}\int_{-\infty}^{+\infty} \mathrm{d}\nu_x \frac{I_{\mathrm{IMF}}(\nu_x,y)}{(x-\nu_x)}, \quad (2)$$

and with respect to the coordinate y,

$$H_y(x,y) = \frac{1}{\pi}\mathrm{PV}\int_{-\infty}^{+\infty} \mathrm{d}\nu_y \frac{I_{\mathrm{IMF}}(x,\nu_y)}{(y-\nu_y)}. \quad (3)$$

The PHT was applied to each row and column of the selected set of 2D IMFs as it is described in Eqs. (2) and (3), and the amplitude of each of these images was calculated using the absolute value of its partial analytic image. The full amplitude image $A(x,y)$ was reconstructed by averaging the previously obtained partial absolute values as

$$A(x,y) = \frac{|I_{\mathrm{IMF}}(x,y) + iH_x(x,y)| + |I_{\mathrm{IMF}}(x,y) + iH_y(x,y)|}{2}. \quad (4)$$

The reason for using the PHT in this work instead of other 2D transforms, such as the spiral quadrature transform, was based on the consideration that the modulation amplitude and not the phase was under computation. Therefore, the mentioned x and y Hilbert transforms worked very well for our purpose.

Once the amplitude $A(x,y)$ of the representative group of 2D IMFs was calculated, the normalized pattern was obtained by dividing $I_{\mathrm{IMF}}(x,y)$ by its corresponding amplitude $A(x,y)$. The bias suppression was achieved keeping only the significant 2D IMFs, since the bias component information lies in the last modes of the decomposition. The number of significant 2D IMFs to be selected was the only step of the normalization procedure that needed external supervision. This number can vary depending on the fringe patterns to be normalized. In most cases, the first 2D IMF was enough to perform the normalization. However, when the fringe patterns contained a wide range of frequency information, it could be necessary to use the second, and sometimes the third, 2D IMF as well.

3. Numerical Evaluation

The computer simulated fringe patterns used to evaluate the normalization technique were generated with added illumination defects in the form of Gaussian shaped bias components and modulation distortions. The Gaussian defects had different variance and were centered at various regions of the fringe patterns to simulate different types of distortions. The fringes were generated for a resolution of 128 × 128 pixels with 256 gray levels. This approach allows

one to know precisely the original fringe pattern and the introduced distortions, so that a figure of merit can be used to evaluate the proposed normalization technique.

The performance of the normalization technique was obtained by calculating a figure of merit, named the quality index Q, to avoid the weak performance that exhibits the mean-square-error criterion commonly accepted in the literature. The index Q compares the normalized fringe patterns with the defect-free ones, and it is defined as [25]

$$Q \equiv \frac{4\sigma_{EO}\bar{E}\bar{O}}{(\sigma_E^2+\sigma_O^2)[\bar{E}^2+\bar{O}^2]}, \tag{5}$$

where O is the defect-free image and E is the normalized fringe pattern. $\bar{E}$, σ_E and $\bar{O}$, σ_O are the means and the standard deviations of the normalized fringe pattern and the defect-free image, respectively, and σ_{EO} is the covariance between E and O. The Q index allows one to model distortions of any kind as a combination of loss of correlation and luminance and contrast distortions as it can be deduced from Eq. (5),

$$Q = \frac{\sigma_{EO}}{\sigma_E\sigma_O}\frac{2\bar{E}\,\bar{O}}{(\bar{E})^2+(\bar{O})^2}\frac{2\sigma_E\sigma_O}{\sigma_E^2+\sigma_O^2}. \tag{6}$$

The dynamic range of the Q index is $[-1,1]$, and $Q=1$ is the best value that could be achieved. The index was calculated using a sliding window of 5×5 pixels that was displaced pixel by pixel across the horizontal and vertical directions of the image, and the final result was obtained as the mean of the previously computed values.

It should be noted that the processing time required by the proposed normalization algorithm is quite limited. It takes between approximately 1 and 2 min to normalize a fringe pattern with a resolution of 512×512 pixels using MatLab version 7.0 with a 1.8 GHz Intel Core 2 Duo personal computer.

As a typical example, Fig. 1(a) shows a very simple computer-simulated fringe pattern with a low fringe density, and a Gaussian bias and modulation defects. Figure 1(b) displays the normalized image obtained with the technique proposed in this paper by using only the first 2D IMF of the decomposition process. The value of the Q index calculated for this fringe pattern was $Q=0.764$. Figure 2(a) shows a more complex example with the same modulation defects as in Fig. 1(a). The normalized fringes are shown in Fig. 2(b) with a Q index value of 0.898. In this example, the first 2D IMF in the normalization process was also used. Figures 1(b) and 2(b) clearly show the effectiveness of the proposed normalization approach.

The results of normalizing fringe patterns using BEMD and the PHT were also compared with those obtained by the application of the technique proposed in Ref. [2]. Figure 3(a) shows a computer-simulated fringe pattern similar to the one depicted in Fig. 2(a), although with a higher fringe density and a higher modulation variation. Figures 3(b) and 3(c) display the results of applying the BEMD and the PHT approach and the two orthogonal bandpass filter method of Ref. [2], respectively. It is observed that Fig. 3(c) presents defects in the low modulation area of the image, while the normalized fringe pattern obtained from the BEMD and PHT techniques is free of defects [$Q=0.845$ for Fig. 3(b) and $Q=0.160$ for Fig. 3(c)].

To illustrate the performance of the proposed technique, Figs. 4(a)–4(c) also display the intensity profile along the middle row corresponding to Figs. 3(a)–3(c), respectively. Figure 4(b) shows the normalization effect produced by the use of the proposed technique, which can also remove the excessive

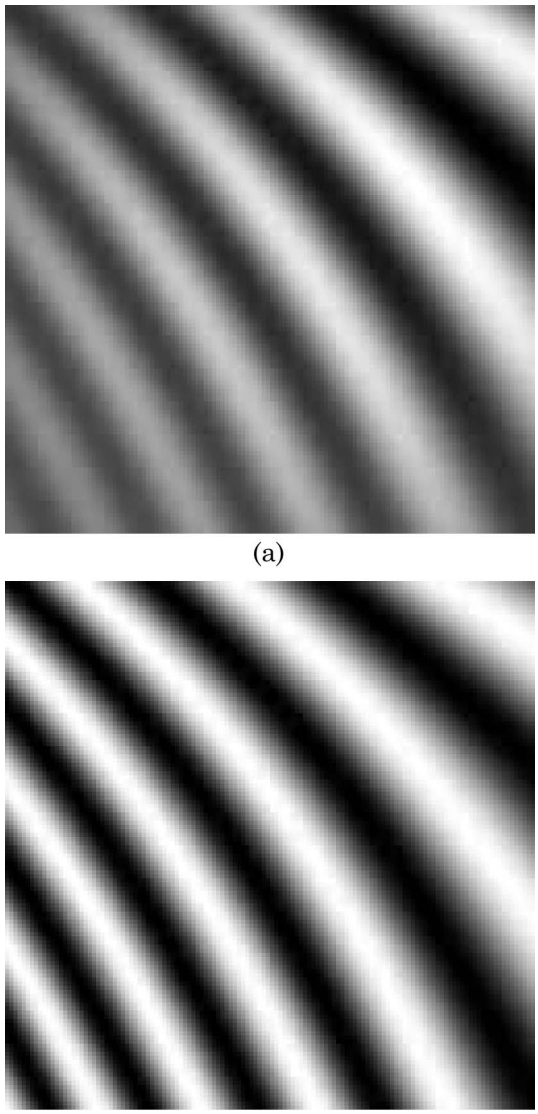

Fig. 1. Normalization of a low frequency computer-generated fringe pattern: (a) fringe pattern containing a bias component and a modulation defect, (b) normalized fringe pattern obtained using the first 2D IMF ($Q=0.764$).

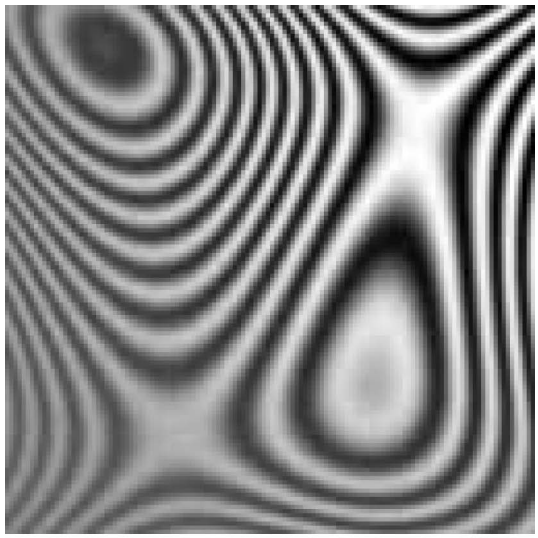

(a)

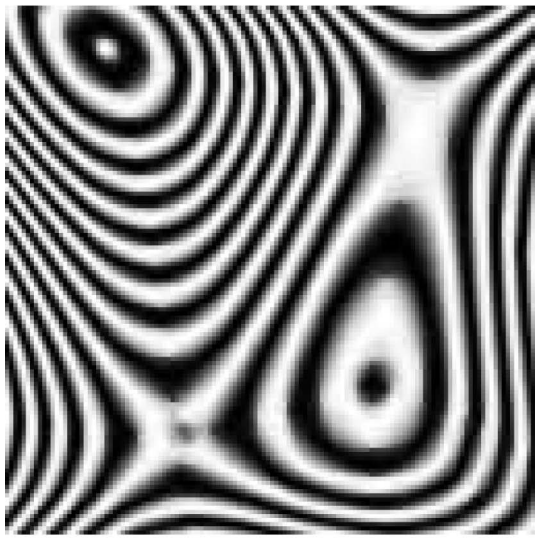

(b)

Fig. 2. Normalization of a more complex computer-generated fringe pattern: (a) fringe pattern containing a bias component and a modulation defect, (b) normalized fringe pattern obtained using the first 2D IMF ($Q = 0.898$).

bias depicted in Fig. 4(a). Note that the bias was removed in Fig. 4(c), although the normalization process could not be completed.

Figure 5 presents an example of bias removal and modulation normalization applied to a computer-simulated DPSI fringe pattern generated using the method presented in Ref. [26]. Figure 5(a) shows the original DSPI fringe pattern, which contains high levels of speckle noise, and Fig. 5(b) displays the smoothed pattern obtained by applying the wave atoms speckle reduction method proposed in Ref. [11]. It can be seen that the denoised image presents modulation defects introduced by the denoising procedure. Figure 5(c) shows the result of applying the proposed normalization technique to the fringe pattern of Fig. 5(b) with a Q index value of 0.842.

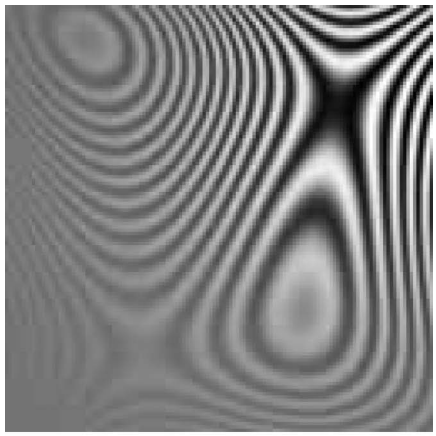

(a)

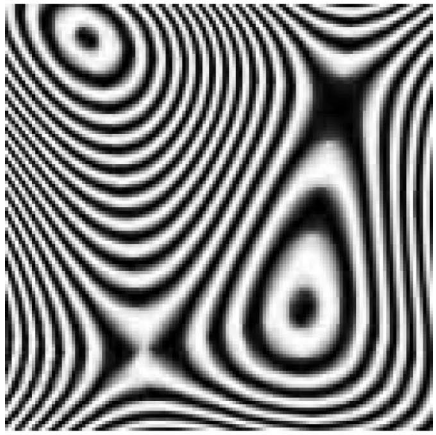

(b)

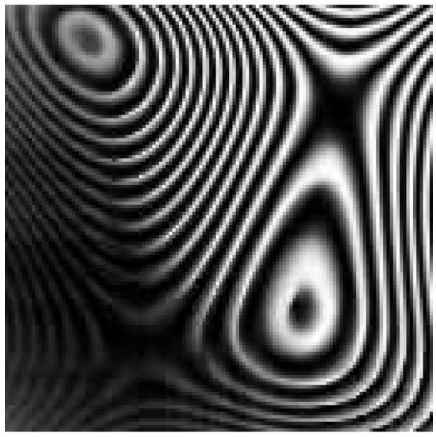

(c)

Fig. 3. Comparison between the proposed technique and another normalization method: (a) fringe pattern containing a bias component and a modulation defect, (b) normalized fringe pattern obtained using the first 2D IMF ($Q = 0.845$), (c) fringe pattern normalized using the two orthogonal bandpass filter method of Ref. [2] ($Q = 0.160$).

4. Experimental Results

To illustrate the performance of the proposed normalization method when experimental data are processed, we analyzed real DSPI fringes recorded from the study of a metal plate subjected to a thermal load

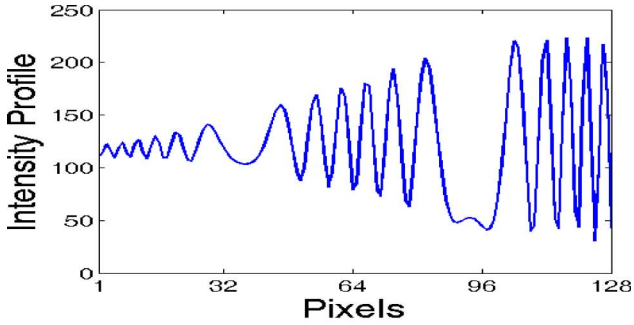

(a)

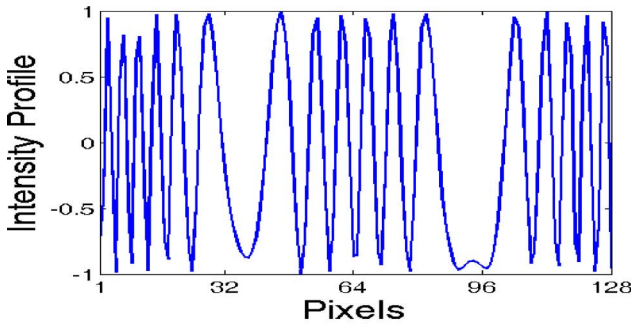

(b)

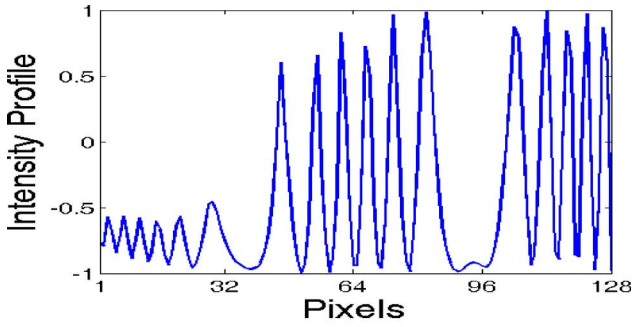

(c)

Fig. 4. (Color online) Intensity profiles along the middle row of the fringe patterns depicted in Fig. 3: (a) original fringe pattern, (b) fringe pattern normalized with the proposed method, (c) fringe pattern normalized with the two orthogonal bandpass filter technique of Ref. [2].

[27]. Figure 6(a) shows a typical fringe pattern, which represents the out-of-plane displacement field generated by the plate when it was heated with an infrared lamp from its back surface. The deformations of the fringes displayed at the top and bottom of the image correspond to the presence of two flat-bottomed holes that were milled into the back surface to simulate internal flaws. This figure clearly shows the defect displayed in the fringe pattern caused by the nonuniform illumination.

Figure 6(b) displays the denoised fringe pattern generated with the speckle smoothing technique presented in Ref. [14], which contains modulation defects generated by the denoising procedure. The normalized image obtained from Fig. 6(b) by the application of the proposed normalization technique when the first two 2D IMFs were used, is shown

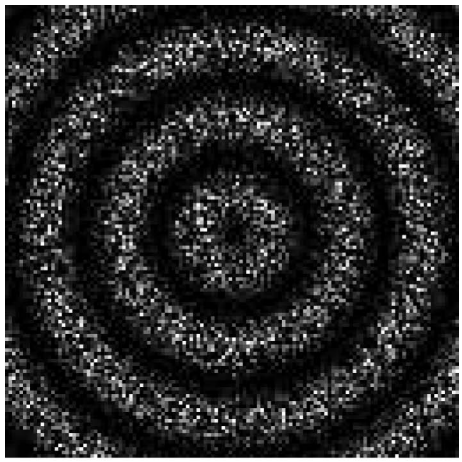

(a)

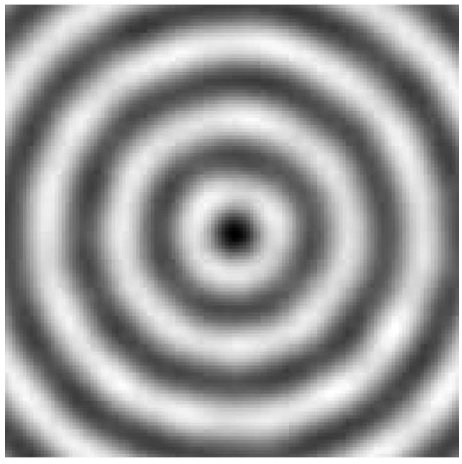

(b)

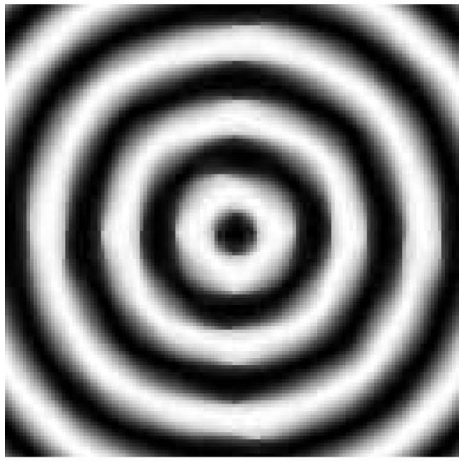

(c)

Fig. 5. Computer-generated DSPI fringe pattern: (a) original fringe pattern, (b) smoothed fringe pattern obtained using the wave atoms technique of Ref. [11] containing modulation defects introduced by the denoising procedure, (c) fringe pattern normalized with the proposed method using the first 2D IMF ($Q = 0.842$).

in Fig. 6(c). As a comparison, Fig. 6(d) depicts the result of applying the two orthogonal bandpass filter method of Ref. [2] to the denoised image of Fig. 6(b). Figure 6(c) shows that the modulation defects are

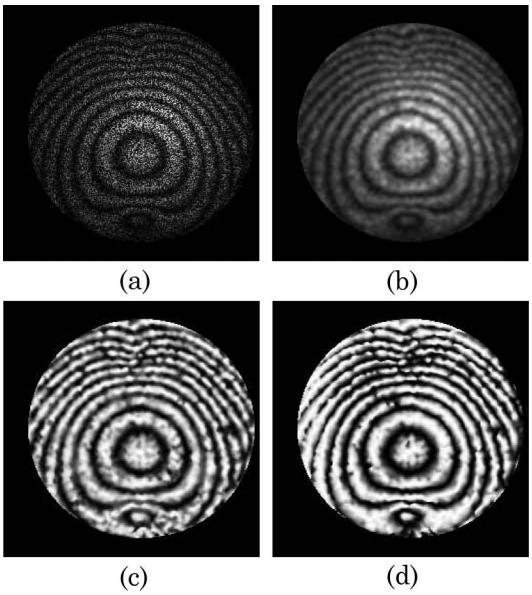

Fig. 6. Experimental DSPI fringe pattern containing an illumination defect: (a) original fringe pattern, (b) fringe pattern denoised using the BEMD method, (c) fringe pattern normalized with the proposed technique using the first two 2D IMFs, (d) fringe pattern normalized with the two orthogonal bandpass filter technique of Ref. [2].

removed while the structure of the fringes is preserved. In addition, the deformation of the fringes due to the two flaws are still clearly observable.

5. Conclusions

This paper evaluates a bias removal and a normalization data-driven technique to be used in fringe pattern analysis. The proposed technique is based on the BEMD method and the PHT. The performance of the normalization technique was tested in computer-simulated fringe patterns with low and high fringe densities and also in real data. Illumination defects of varying intensities were added at different locations of the fringe patterns to evaluate the bias removal and the modulation normalization. The performance of the technique was evaluated using a quality index Q. Good results were obtained in all the evaluated cases, even in fringe patterns with very low modulation regions and stepped contrast changes. It was also noted that the proposed technique is more accurate when it is applied to fringe patterns with high fringe densities. As the last 2D IMFs of the decomposition contain the bias component, it can be removed automatically without using any other preprocessing. Moreover, as BEMD is an adaptive technique that allows the decomposition of complex fringe patterns with nonlinear and nonstationary data in simpler components, the normalization of fringe patterns having a wide range of frequency information and varying geometry is facilitated. Besides, since BEMD is based on local characteristics of the data, the proposed normalization technique presents no difficulties in the normalization of fringes with extremely low modulation areas or contrast changes presenting a high variation.

M. B. Bernini would like to acknowledge the financial support provided by Fundación Josefina Prats of Argentina.

References

1. D. Malacara, M. Servin, and Z. Malacara, *Interferogram Analysis for Optical Testing* (Marcel Dekker, 1998).
2. J. A. Quiroga, J. A. Gómez-Pedrero, and A. García-Botella, "Algorithm for fringe pattern normalization," Opt. Commun. **197**, 43–51 (2001).
3. J. A. Quiroga and M. Servin, "Isotropic n-dimensional fringe pattern normalization," Opt. Commun. **224**, 221–227 (2003).
4. R. Legarda-Sáenz, W. Osten, and W. Jüptner, "Improvement of the regularized phase tracking technique for the processing of nonnormalized fringe patterns," Appl. Opt. **41**, 5519–5526 (2002).
5. P. K. Rastogi, *Digital Speckle Pattern Interferometry and Related Techniques* (Wiley, 2001).
6. L. Watkins, S. Tan, and T. Barnes, "Determination of interferometer phase distributions by use of wavelets," Opt. Lett. **24**, 905–907 (1999).
7. C. A. Sciammarella and T. Kim, "Determination of strains from fringe patterns using space-frequency representations," Opt. Eng. **42**, 3182–3193 (2003).
8. A. Federico and G. H. Kaufmann, "Phase retrieval in digital speckle pattern interferometry using a smoothed time-frequency distribution," Appl. Opt. **42**, 7066–7071 (2003).
9. A. Federico and G. H. Kaufmann, "Phase retrieval in digital speckle pattern interferometry by application of two-dimensional active contours called snakes," Appl. Opt. **45**, 1909–1916 (2006).
10. A. Federico and G. H. Kaufmann, "Local denoising of digital speckle pattern interferometry fringes using multiplicative correlation and weighted smoothing splines," Appl. Opt. **44**, 2728–2735 (2005).
11. A. Federico and G. H. Kaufmann, "Denoising in digital speckle pattern interferometry using wave atoms," Opt. Lett. **32**, 1232–1234 (2007).
12. J. A. Guerrero, J. L. Marroquin, M. Rivera, and J. A. Quiroga, "Adaptive monogenic filtering and normalization of ESPI fringe patterns," Opt. Lett. **30**, 3018–3020 (2005).
13. N. A. Ochoa and A. A. Silva-Moreno, "Normalization and noise-reduction algorithm for fringe patterns," Opt. Commun. **270**, 161–168 (2007).
14. M. B. Bernini, A. Federico, and G. H. Kaufmann, "Noise reduction in digital speckle pattern interferometry using bidimensional empirical mode decomposition," Appl. Opt. **47**, 2592–2598 (2008).
15. N. E. Huang, Z. Sheng, S. R. Long, M. C. Wu, H. H. Shih, Q. Zheng, N. C. Yen, C. C. Tung, and H. H. Liu, "The empirical mode decomposition and the Hilbert spectrum for non-linear and non-stationary time series analysis," Proc. R. Soc. London Ser. A **454**, 903–995 (1998).
16. C. Damerval, S. Meignen, and V. Perrier, "A fast algorithm for bidimensional EMD," IEEE Signal Process Lett. **12**, 701–704 (2005).
17. H. T. Yang, *Finite Element Structural Analysis* (Prentice-Hall, 1986).
18. Y. Tian, Y. Huang, and Y. Li, "Image zooming method using 2D EMD technique," in *Proceedings of IEEE 6th World Congress on Intelligent Control and Automation* (IEEE, 2006), pp. 10036–10040.
19. K. Zeng and M. He, "A simple boundary process technique for empirical mode decomposition," in *Proceedings of IEEE*

Geoscience and Remote Sensing Symposium (IEEE, 2004), Vol. 6, pp. 4258–4261.
20. G. Rilling, P. Flandrin, and P. Gonçalves, "On empirical mode decomposition and its algorithms," in *Proceedings of IEEE-EURASIP Workshop on Nonlinear Signal and Image Processing* (IEEE, 2003) (http://perso.ens-lyon.fr/paulo.goncalves/index.php?page=Publications=emd-eurasip03#Communications).
21. Z. Liu and S. Peng, "Boundary processing of bidimensional EMD using texture synthesis," IEEE Signal Process Lett. **12**, 33–36 (2005).
22. M. Shen, H. Tang, and B. Li, "The modified bidimensional empirical mode decomposition for image denoising," in *Proceedings of IEEE 8th International Conference on Signal Processing* (IEEE, 2006), pp. 16–20.
23. W. Press, S. Teukolsky, W. Vetterling, and B. Flannery, *Numerical Recipes in C*, 2nd ed. (Cambridge Univ. Press, 1992), Chap. 13.
24. S. L. Hahn, *Hilbert Transforms in Signal Processing* (Artech House, 1996).
25. Z. Wang and A. C. Bovik, "A universal quality index," IEEE Signal Process Lett. **9**, 81–84 (2002).
26. P. D. Ruiz and G. H. Kaufmann, "Evaluation of a scale-space filter for speckle noise reduction in electronic speckle pattern interferometry," Opt. Eng. **37**, 2395–2401 (1998).
27. G. H. Kaufmann, "Nondestructive testing with thermal waves using phase shifted temporal speckle pattern interferometry," Opt. Eng. **42**, 2010–2014 (2003).